RSC Advances

PAPER

View Article Online
View Journal | View Issue

Check for updates

Cite this: *RSC Adv.*, 2020, **10**, 4243

Cytotoxic alkaloids from the marine shellfish-associated fungus *Aspergillus* sp. XBB-4 induced by an amino acid-directed strategy†

Yi Qiu,[a] Qi Guo,[a] Yan-Qin Ran,[b] Wen-Jian Lan,[c] Chi-Keung Lam,[a] Gong-Kan Feng,[d] Rong Deng,[d] Xiao-Feng Zhu,[d] Hou-Jin Li*[a] and Liu-Ping Chen*[a]

Received 9th December 2019
Accepted 20th January 2020

DOI: 10.1039/c9ra10306f

rsc.li/rsc-advances

Eight different culture media were used to culture shellfish *Panopea abbreviate* associated fungus *Aspergillus* sp. XBB-4. In a glucose-peptone-yeast (GPY) culture medium supplied with amino acids, this fungus can produce chemodiversity metabolites. Four new alkaloids including three β-carboline alkaloids, aspercarbolines A–C (**1–3**) and one piperazinedione, asperdione A (**13**) along with nine known compounds were isolated. The structures were elucidated mainly based on the NMR, MS, ECD and X-ray single-crystal diffraction data. The possible biosynthetic pathways of aspercarbolines A–C (**1–3**) were proposed. All compounds (**1–13**) were evaluated for their cytotoxicity against six cancer cell lines, including human nasopharyngeal carcinoma cell lines CNE1, CNE2, HONE1 and SUNE1, and human hepatocellular carcinoma cell lines hepG2 and QGY7701.

Open Access Article. Published on 27 January 2020. Downloaded on 2/21/2026 1:43:14 AM.
This article is licensed under a Creative Commons Attribution-NonCommercial 3.0 Unported Licence.

Introduction

Currently, the demand for seafood across the world is increasing owing to a wide range of health benefits in it. For example, appropriate consumption of seafood can reduce the risk of developing coronary heart disease (CHD), high blood pressure, stroke, some cancers, rheumatoid arthritis and other inflammatory diseases.[1] However, seafood allergy becomes a serious health problem at the same time as the data shows that up to 2.5% of the general population suffers worldwide.[2] The occurrence of seafood allergy may be aroused due to two factors: some seafood especially shellfish are filter feeders and selectively accumulate microorganisms from surrounding waters. Then they are normally eaten whole, without removing the intestinal tract, and raw or just with a very mild heat treatment.[3]

Geoduck *Panopea abbreviate* is a kind of important economic shellfish and many research studies about it have been reported. For instance, P. C. Zaidman and E. Morsan studied the growth variability of geoduck in a metapopulation.[4] M. Goman *et al.* tested the suitability of using geoduck shells to evaluate changes in both annual and seasonal sea surface temperature, since geoducks are long-lived and deposit well-defined annual growth lines within their shells each winter.[5] Other studies were about the nutritional value of geoducks[6] or how to make the artificial reproduction of them.[7] Few studies were focused on the secondary metabolites from microbial communities which were associated with geoducks.

Recently, a fungal strain *Aspergillus* sp. XBB-4 was isolated from geoduck *Panopea abbreviate* in our laboratory. Our previous studies have shown that systematic alteration of easily accessible cultivation parameters could affect microorganisms' metabolism. For examples, five new triquinane-type sesquiterpenoids chondrosterins A–E were isolated from marine fungus *Chondrostereum* sp. cultured in PDB (potato dextrose broth) medium[8] and 14 new alkaloids were obtained from marine fungus *Scedosporium apiospermum* F41-1 cultured in GPY (glucose peptone yeast) medium contained a variety of amino acids.[9] Two new bisindole compounds, pseudboindoles A and B, together with 11 known indole alkaloids were efficiently isolated from the marine fungus *Pseudallescheria boydii* F44-1 which was cultured in GPY medium with an amino acid-directed strategy by Yuan *et al.*[10] Therefore, in order to optimize the culture conditions of this fungal strain, eight different culture media were developed. Finally, according to the LC-MS spectra of their culture extracts, the fungal strain

[a]*School of Chemistry, Sun Yat-sen University, Guangzhou 510275, China. E-mail: ceslhj@mail.sysu.edu.cn; cesclp@mail.sysu.edu.cn*
[b]*School of Traditional Chinese Medicine, Guangdong Pharmaceutical University, Guangzhou 510006, China*
[c]*School of Pharmaceutical Sciences, Sun Yat-sen University, Guangzhou 510006, China*
[d]*State Key Laboratory of Oncology in South China, Collaborative Innovation Center for Cancer Medicine, Cancer Center, Sun Yat-sen University, Guangzhou 510060, China*

† Electronic supplementary information (ESI) available: HRESIMS, 1D and 2D NMR spectra of compounds **1–3** and **13**; 1D NMR spectra of compounds **4–12**; ECD calculation of compounds **1**, **3** and **13**; crystallographic data of compound **13**; composition of each nutrient source in eight culture media and HPLC spectra of extracts from eight culture media. CCDC 1969177. For ESI and crystallographic data in CIF or other electronic format see DOI: 10.1039/c9ra10306f

Open Access Article. Published on 27 January 2020. Downloaded on 2/21/2026 1:43:14 AM.
This article is licensed under a Creative Commons Attribution-NonCommercial 3.0 Unported Licence.

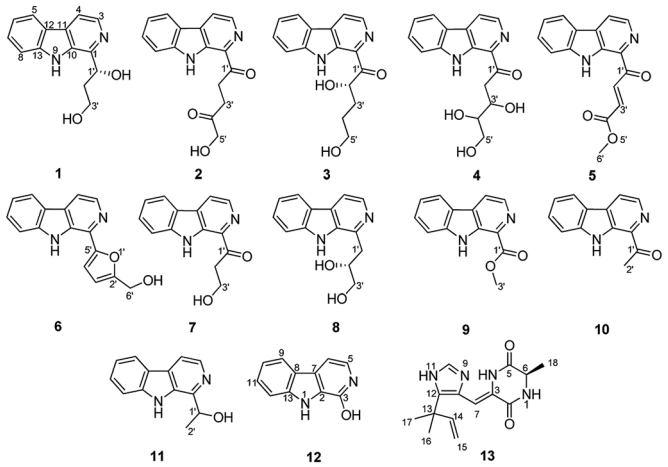

Fig. 1 Chemical structures of compounds **1–13**.

cultured in GPY + amino acids produced the alkaloids metabolites with chemodiversity. So the fungus *Aspergillus* sp. XBB-4 was cultured in GPY + amino acids medium on a large scale. Metabolites investigation resulted in the isolation and structural determination of **13** compounds, including three new β-carboline alkaloids, aspercarbolines A–C (**1–3**), one new piperazinedione, asperdione A (**13**) and nine known compounds (Fig. 1). Herein, the isolation, structure characterization, proposed biosynthetic pathway and cytotoxic activity of these compounds were reported.

Results and discussion

Structural elucidation

Aspercarboline A (**1**) was isolated as a brown oil. Its molecular formula was determined to be $C_{14}H_{14}N_2O_2$ by HR-ESI-MS at *m*/*z* 243.11268 $[M + H]^+$ (calcd for $C_{14}H_{15}N_2O_2$, 243.11280), having nine degrees of unsaturation (ESI Fig. S1†). The ^{13}C NMR spectrum of **1** indicated the presences of **11** aromatic carbons and three aliphatic carbons, which could be classified to five quaternary carbons, seven methines and two methylenes according to the DEPT spectra (ESI Fig. S3–S5†). The diagnostic aryl proton signals at δ_H 8.21 (d, 8.0, H-5), 7.71 (d, 8.0, H-8), 7.54 (dd, 8.0, 1.0, H-7) and 7.25 (dd, 8.0, 1.0, H-6) along with the ^1H–^1H COSY correlations of H-5/H-6, H-6/H-7 and H-7/H-8 suggested a 1,2-disubstituted benzene ring in this molecule (Table 1 and ESI Fig. S2†). The ^1H–^1H COSY spectrum also indicated the presence of a pair of aromatic protons H-3 (δ_H 8.28, d, 5.0) and H-4 (δ_H 7.98, d, 5.0) (ESI Fig. S7†). The HMBC correlations from H-3 to C-1 (δ_C 148.3) and C-11 (δ_C 129.9); from H-4 to C-10 (δ_C 133.9), C-11 and C-12 (δ_C 122.0); from H-5 to C-7 (δ_C 128.9); from H-6 to C-8 (δ_C 113.0) and C-13 (δ_C 141.7); from H-7 to C-5 (δ_C 122.2), C-6 and C-8; from H-8 to C-6 and C-13 displayed a β-carboline fragment (Fig. 2 and ESI Fig. S8†). The ^1H–^1H COSY and HSQC spectra along with the molecular formula showed that **1** had two hydroxyl groups (δ_H 5.15, s; 4.03, s) (ESI Fig. S6†). The ^1H–^1H COSY cross-peaks of H-2′/H-1′, H-2′/H-3′ and the HMBC correlations from H-2′ to C-1′ and C-1, from H-3′ to C-2′ revealed the side chain –CH(OH)CH_2CH_2OH was connected to C-1. The absolute configuration of **1** was defined

Table 1 ^1H and ^{13}C NMR data for **1–3** (δ in ppm)

	1 (in acetone-d_6)[a]		**2** (in $CDCl_3$)[b]		**3** (in DMSO-d_6)[b]	
No.	δ_C, type	δ_H, mult. (*J* in Hz)	δ_C, type	δ_H, mult. (*J* in Hz)	δ_C, type	δ_H, mult. (*J* in Hz)
1	148.3, C		135.6, C		135.8, C	
3	138.0, CH	8.28, d (5.0)	138.4, CH	8.54, d (4.8)	137.3, CH	8.49, d (4.8)
4	114.2, CH	7.98, d (5.0)	119.5, CH	8.17, d (4.8)	119.2, CH	8.41, d (4.8)
5	122.2, CH	8.21, d (8.0)	122.0, CH	8.15, d (8.0)	121.7, CH	8.29, d (8.0)
6	120.3, CH	7.25, dd (8.0, 1.0)	121.0, CH	7.34, dd (8.0, 1.2)	120.1, CH	7.29, dd (8.0, 1.2)
7	128.9, CH	7.54, dd (8.0, 1.0)	129.5, CH	7.60, dd (8.0, 1.2)	128.8, CH	7.58, dd (8.0, 1.2)
8	113.0, CH	7.71, d (8.0)	112.1, CH	7.57, d (8.0)	113.0, CH	7.80, d (8.0)
9-NH		10.63, s		10.18, s		11.90, s
10	133.9, C		135.3, C		134.0, C	
11	129.9, C		131.8, C		130.9, C	
12	122.0, C		120.8, C		119.8, C	
13	141.7, C		141.3, C		141.8, C	
1′	73.3, CH	5.37, dd (8.0, 4.0)	202.8, C		203.5, C	
2′	40.5, CH_2	2.21, m; 2.11, m	32.2, CH_2	3.85, t (6.4)	70.7, CH	3.56, m
3′	60.4, CH_2	3.87, dt (10.5, 6.0); 3.80, dt (10.5, 6.0)	32.3, CH_2	2.89, t (6.4)	28.0, CH_2	1.96, m; 1.69, m
4′			208.9, C		33.6, CH_2	3.42, m
5′			68.5, CH_2	4.47, s	65.9, CH_2	3.36, m
1′-OH		5.15, s				
2′-OH						4.55, d (5.2)
3′-OH		4.03, s				
5′-OH				3.13, s		4.50, t (5.6)

[a] ^1H and ^{13}C NMR data were recorded at 500/125 MHz, respectively. [b] ^1H and ^{13}C NMR data were recorded at 400/100 MHz, respectively.

 This journal is © The Royal Society of Chemistry 2020

Open Access Article. Published on 27 January 2020. Downloaded on 2/21/2026 1:43:14 AM.
This article is licensed under a Creative Commons Attribution-NonCommercial 3.0 Unported Licence.

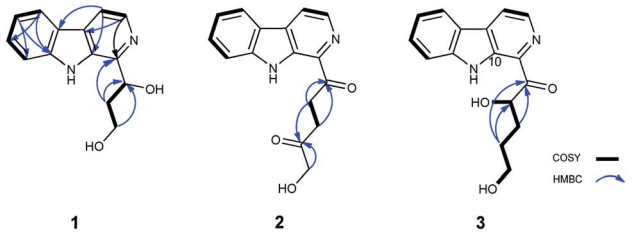

Fig. 2 $^{1}H-^{1}H$ COSY (bold lines), main HMBC (blue arrows) correlations of compounds **1–3**.

by comparison of the experimental and calculated ECD data. The calculated ECD curve of 1′*R*-1 was well matched with the experimental curve (Fig. 3). Therefore, the absolute configuration of **1** was defined as 1′*R*. The chemical structure of aspercarboline A (**1**) was unambiguously established, as shown in Fig. 1.

Aspercarboline B (**2**) was obtained as a white powder and its molecular formula was established as $C_{16}H_{14}N_2O_3$ by HR-ESI-MS at *m*/*z* 283.10891 $[M + H]^+$ (calcd for $C_{16}H_{15}N_2O_3$, 283.10772) requiring 11 degrees of unsaturation (ESI Fig. S9†). After careful comparison of the ^{1}H and ^{13}C NMR spectra, compound **2** was found to possess similar signals to compound **1** in the aromatic region, so compound **2** was quickly identified as a β-carboline alkaloid having different side chain (ESI Fig. S10 and S11†). The ^{13}C NMR and DEPT spectra revealed two carbonyl carbons (δ_C 202.8 and 208.9) and three methylene groups (δ_C 68.5, 32.3 and 32.2) in the side chain (ESI Fig. S12 and S13†). From the HSQC spectrum and the $^{1}H-^{1}H$ COSY correlation between H-2′ (δ_H 3.85, t, 6.4) and H-3′ (δ_H 2.89, t, 6.4) revealed the presence of the fragment $-CH_2CH_2-$ (ESI Fig. S14 and S15†). The remaining methylene group (δ_C 68.5, δ_H 4.47, s) was deduced to connect to the hydroxyl group (δ_H 3.13, s). The HMBC correlations of H-2′/C-1′ (δ_C 202.8), H-2′/C-4′ (δ_C 208.9), H-3′/C-1′, H-3′/C-4′, and H-5′/C-4′ elucidated the side chain as $-C(=O)CH_2CH_2C(=O)CH_2OH$ (ESI Fig. S16†).

Aspercarboline C (**3**) was isolated as a white powder. The molecular formula was identified as $C_{16}H_{16}N_2O_3$ based on HR-ESI-MS peak at *m*/*z* 285.12302 $[M + H]^+$ (calcd for $C_{16}H_{17}N_2O_3$, 285.12337) (ESI Fig. S17†), indicating 10 degrees of unsaturation. Its similar ^{1}H and ^{13}C NMR spectra signals to compound **1**

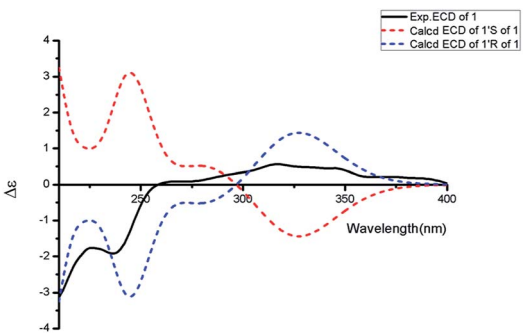

Fig. 3 Experimental ECD spectrum in MeOH and the calculated ECD spectra of compound **1**.

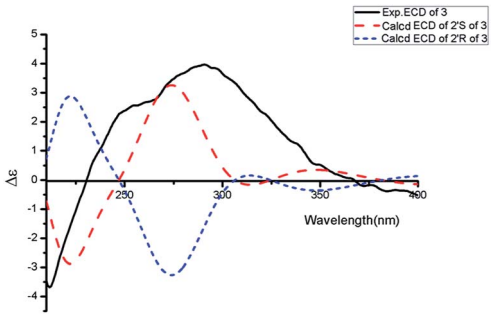

Fig. 4 Experimental ECD spectrum in MeOH and the calculated ECD spectra of compound **3**.

in the aromatic region, suggested a β-carboline alkaloid as well (ESI Fig. S18 and S19†). Based on the analysis of the ^{13}C NMR and DEPT spectra, three methylenes, one methine and one quaternary carbon were contained at the side chain (ESI Fig. S20†). The quaternary carbon at δ_C 203.5 (C-1′) revealed a ketone carbonyl. From the $^{1}H-^{1}H$ COSY correlations of H-2′ (δ_H 3.56)/H-3′ (δ_H 1.69, 1.96)/H-4′ (δ_H 3.42)/H-5′ (δ_H 3.36), H-2′/2′-OH (δ_H 4.55) and H-5′ (δ_H 3.36)/5′-OH (δ_H 4.50), the fragment of $-CH(OH)CH_2CH_2CH_2OH$ was established (Fig. 2 and ESI Fig. S22†). Moreover, the HMBC correlations (ESI Fig. S23†) from H-3′ to C-1′ and H-4′ to C-1′ demonstrated that the carbonyl group (C-1′) was linked with C-1 (δ_C 135.8) and C-2′ (δ_C 70.7) to connect the long side chain and the β-carboline skeleton. The absolute configuration of **3** was defined as 2′*S* because the calculated ECD curve of 2′*S*-3 was almost consistent with the experimental one (Fig. 4). Finally, the structure of **3** was established as shown in Fig. 1.

Asperdione A (**13**) was obtained as colorless crystals with the molecular formula $C_{14}H_{18}N_4O_2$ determined by the HR-ESI-MS peak at *m*/*z* 275.15079 $[M + H]^+$ (calcd for

Table 2 ^{1}H (600 MHz) and ^{13}C NMR (150 MHz) data for **13** in $CDCl_3$ (δ in ppm)

No.	δ_C, type	δ_H, mult. (*J* in Hz)
1	NH	9.13, s
2	160.2, C=O	
3	132.4, C	
4	NH	7.55, s
5	166.1, C=O	
6	51.9, CH	4.26, q (7.2)
7	105.4, CH	6.93, s
8	124.3, C	
9	N	
10	132.5, CH	6.02, brs
11	NH	11.95, s
12	136.8, C	
13	37.8, C	
14	144.8, CH	6.04, dd (17.4, 10.8)
15	113.6, CH_2	5.20, d (17.4); 5.17, d (10.8)
16	28.1, CH_3	1.51, s
17	28.1, CH_3	1.51, s
18	21.5, CH_3	1.57, d (7.2)

Open Access Article. Published on 27 January 2020. Downloaded on 2/21/2026 1:43:14 AM.
This article is licensed under a Creative Commons Attribution-NonCommercial 3.0 Unported Licence.

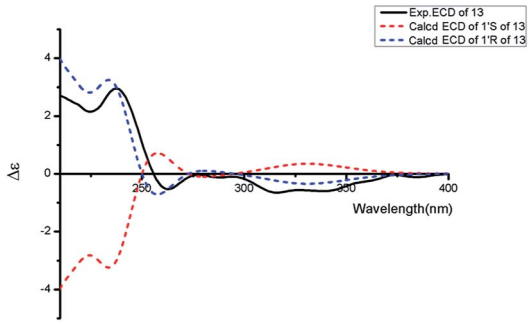

Fig. 5 Experimental ECD spectrum in MeOH and the calculated ECD spectra of compound **13**.

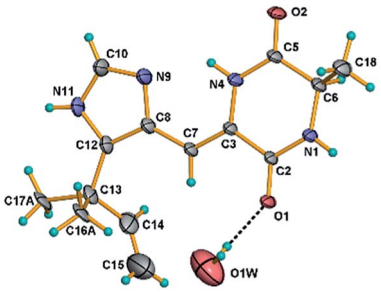

Fig. 7 ORTEP diagram for the single-crystal X-ray structure of compound **13**.

$C_{14}H_{19}N_4O_2$, 275.15025), indicating the presence of 4 degrees of unsaturation (ESI Fig. S24†). In the ^{1}H NMR spectrum of **13**, there was a peak (δ_H 1.51) (Table 2) in the upfield whose integral was 6.00 (ESI Fig. S25†). It suggested that **13** might have two same methyl groups which was confirmed by the observation of a peak (δ_C 28.1) in the ^{13}C NMR spectrum whose signal was almost double strong as the other peaks (ESI Fig. S26†). From the ^{13}C NMR and DEPT spectra, C-2 (δ_C 160.2) and C-5 (δ_C 166.1) could be defined as two carbonyl groups (ESI Fig. S27 and S28†). The ^{1}H–^{1}H COSY cross peak of H-6 (δ_H 4.26, q, 7.2, 1H)/H-18 (δ_H 1.57, d, 7.2, 3H) and C-6 (δ_C 51.9) deduced a –CHCH$_3$ fragment was attached to –NH group (ESI Fig. S30†). The HMBC correlations from H-18 to C-5 (δ_C 166.1) and C-6; H-6 to C-2, C-5 and C-18 (δ_C 21.5); H-7 to C-2, C-3 (δ_C 132.4), C-8 (δ_C 124.3) and C-12; and H-4 to C-3, C-8 and C-12 demonstrated the presence of piperazinedione skeleton (Fig. 6 and ESI Fig. S31†). The ^{1}H–^{1}H COSY correlation of H-14 (δ_H 6.04) and H-15 (δ_H 5.17 and 5.20) along with the HMBC correlations from H-16 and H-17 to C-12, C-13, C-14 and C-15; H-15 to C-12, C-13 and C-14; and H-14 to C-12, C-13, C-16 and C-17 presented the fragments of –C–C(CH$_3$)$_2$CH=CH$_2$. Thus, the planar structure of **13** was elucidated (Fig. 1). The absolute configuration of **13** was defined by comparison of the experimental and calculated ECD data. The calculated ECD curve of 6*R*-13 was well matched with the experimental curve (Fig. 5). In addition of the X-ray single crystal diffraction analysis, the absolute configuration of **13** was defined as 6*R* (Fig. 7). Compound **13** is the configuration isomer of a known compound, 3-[[5-(1,1-dimethyl-2-propen-1-yl)-1*H*-imidazol-4-yl]methylene]-6-methyl-(6*S*)-2,5-piperazinedione which was synthesized by E. Couladouros, *et al.* in 2005 (ref. 11) and was isolated as a natural product for the first time by P. Phainuphong *et al.* in 2018.[12]

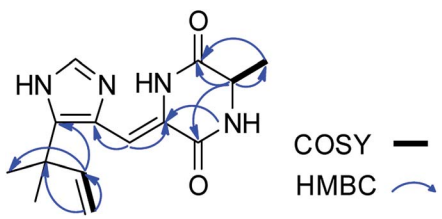

Fig. 6 ^{1}H–^{1}H COSY (bold lines), main HMBC (blue arrows) correlations of compound **13**.

The other compounds were identified as 1-(1-oxo-3,4,5-trihydroxy-1-pentyl)-β-carboline (**4**),[13] 4-(9*H*-β-carbolin-1-yl)-4-oxobut-2-enoic acid methyl ester (**5**),[14] perlolyrin (**6**),[15] 1-(9*H*-β-carbolin-1-yl)-3-hydroxy-propan-1-one (**7**),[16] cordysinin E (**8**),[17] 1-methoxycarbonyl-β-carboline (**9**),[18] 1-acetyl-β-carboline (**10**),[19] cordysinin C (**11**),[20] and 3-hydroxy-β-carboline (**12**)[21] based on their NMR and MS data (ESI Fig. S32–S50†) and by comparing with those previously reported in the literatures.

Proposed biosynthetic pathway

Although it was proved that the origin of the indole part of β-carboline alkaloids was from tryptophan, the other counterparts can be derived from different components.[22] Many researches demonstrated that the enzymatic Pictet–Spengler reaction, catalyzed by Pictet–Spenglerase, was one of the characteristics of β-carboline alkaloid biosynthesis.[23–25] Feeding experiments with 5-F-Trp and ^{13}C labeled glucose and acetate revealed that the synthesis of β-carboline involved a Pictet–Spengler cyclization, a decarboxylation and C-ring oxidation process.[26,27] Combining of the published literatures and basic organic synthesis mechanism, the biosynthetic pathway of compounds **1–3** were proposed. For compound **1**, McbB (McbB is an enzyme which was demonstrated to be absolutely essential for β-carboline core construction[26]) catalyzes two substrates to obtain compound **1a** which is utilized in the Pictet–Spengler

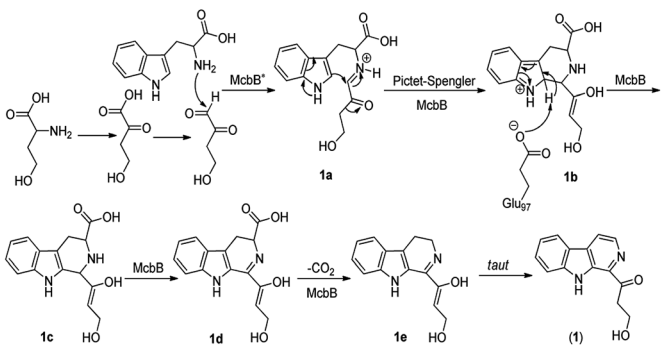

Fig. 8 Proposed biosynthetic pathway of compound **1**.

This journal is © The Royal Society of Chemistry 2020

Open Access Article. Published on 27 January 2020. Downloaded on 2/21/2026 1:43:14 AM.
This article is licensed under a Creative Commons Attribution-NonCommercial 3.0 Unported Licence.

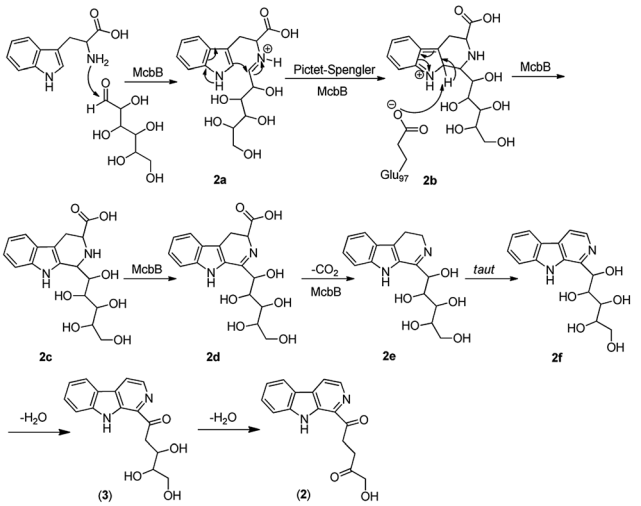

Fig. 9 Proposed biosynthetic pathways of compounds 2 and 3.

cyclization to afford **1b**. The negatively charged Glu97 is used as the active site to complete the C-ring aromatization and then *via* oxidation to product **1d**. **1e** is obtained by decarboxylation from **1d** and followed oxidation lead to the product of compound **1** (Fig. 8). Similarly, the hypothetical biosynthetic pathway of compounds **2** and **3** is given as showed in Fig. 9. Compound **2f** is produced after Pictet–Spengler cyclization, C-ring aromatization, oxidation and decarboxylation. Subsequent elimination of one H_2O from the carbohydrate-derived side chain of **2f** produces compound **3**. Finally, subsequent elimination of one more H_2O from compound **3** obtains compound **2**.

Biological activity

Compounds **1–13** were evaluated for their cytotoxicity against six cancer cell lines, including human nasopharyngeal carcinoma cell lines CNE1, CNE2, HONE1 and SUNE1, human hepatocellular carcinoma cell lines hepG2 and QGY7701 (Table 3). Results showed that compound **3** exhibited a moderate inhibitory effect against all six cell lines except hepG2 with IC_{50} values of 16.29, 20.58, 20.11, 45.31, 50.85 and 28.97 μM. Compound **4** showed moderate cytotoxicity against CNE1, CNE2, HONE1 and QGY7701 with the IC_{50} values from 20.64 to 43.43 μM. Compound **6** presented a strong inhibitory effect against CNE2 with an IC_{50} value of 8.69 μM and moderate inhibitory effects against the other five cell lines. Compounds **7**, **10** and **11** displayed moderate cytotoxicity against QGY7701 with the mean IC_{50} values of 30.40, 35.49 and 49.27 μM respectively while **12** exhibited a strong cytotoxicity to hepG2 and QGY7701. Compound **13** showed potent cytotoxicity against these cancer cell lines with the IC_{50} values ranged from 10.72 to 22.00 μM. In contrast, compounds **1**, **2**, **5**, **8** and **9** were apparently inactive in this assay (IC_{50} > 50 μM). Hirsutanol A was used as a positive control.[28–30]

Table 3 Cytotoxicities of compounds **1–13** against six cancer cell lines, IC_{50} (μM)[a]

Compounds	CNE1	CNE2	HONE1	SUNE1	HepG2	QGY7701
1	95.70	—	77.61	85.94	—	—
2	—	—	84.29	94.05	—	—
3	16.29	20.58	20.11	45.31	50.85	28.97
4	43.31	38.53	42.85	64.95	65.03	20.64
5	60.42	64.04	74.58	70.72	—	51.93
6	22.34	8.69	31.35	23.44	49.79	32.76
7	—	—	—	—	76.53	30.40
8	—	—	—	—	—	—
9	—	—	80.28	—	—	59.40
10	74.67	—	97.39	—	60.13	35.49
11	62.57	—	85.13	—	—	49.27
12	40.58	—	71.16	—	16.93	8.82
13	22.00	18.93	21.61	16.93	12.33	10.72
Hirsutanol A	10.08	12.72	17.40	3.50	10.11	21.12

[a] "–" means ">100".

Experimental

General experimental procedures

The 1D and 2D NMR spectra were obtained on Bruker AV-400, AV-500 and AV-600 spectrometers (Bruker Bio Spin AG, Industriestrasse 26, Fällanden, Switzerland). HR-ESI-MS data were acquired on a Thermo Fisher LTQ Orbitrap Elite high-resolution mass spectrometer (Thermo Fisher Scientific Inc., Waltham, MA, USA). LC-MS data were collected on a Thermo Fisher system (Thermo Fisher Scientific Inc., Waltham, MA, USA) with an Ultimate 3000 RS pump, auto-sampler, diode array detector and column compartment, and coupled with an ISQ EC mass spectrometer. CD spectra were measured on a JASCO J-1700 circular dichroism spectrometer (JASCO International Co. Ltd., Tokyo, Japan). A Shimadzu UV-Vis-NIR spectrophotometer (Shimadzu Corporation, Nakagyo-ku, Kyoto, Japan) was used to obtain UV data. IR spectra were collected on a PerkinElmer Frontier FT-IR spectrophotometer (PerkinElmer Inc., Waltham, MA, USA). Optical rotations were measured using an Anton Paar (MCP 300) polarimeter at 25 °C. X-ray crystallographic analysis was performed on an Agilent Gemini Ultra diffractometer (Cu Kα radiation). Column chromatography was performed with silica gel (SiO_2, 200–300 mesh, Qingdao Marine Chemical Inc., Qingdao, China) and Sephadex LH-20 (GE Healthcare Bio-Sciences, Uppsala, Sweden). Preparative HPLC was performed on a Shimadzu LC-20AT HPLC pump (Shimadzu Corporation, Nakagyo-ku, Kyoto, Japan) and equipped with a SPD-20A dual λ absorption detector (Shimadzu Corporation, Nakagyo-ku, Kyoto, Japan) and a Capcell-Pak C18 UG80 HPLC column (250 mm × 20 mm, Shiseido Co., Ltd., Minato-ku, Tokyo, Japan) added with a Spolar HPLC packed column (250 mm × 4.6 mm, Shiseido Co., Ltd., Minato-ku, Tokyo, Japan).

Fungal material

Aspergillus sp. XBB-4 was isolated from the inner tissue of geoduck *Panopea abbreviate* which was collected from the South China Sea. The sequence data of this fungal strain have been submitted to GenBank with accession number MK863524. This fungal strain was stored at School of Chemistry, Sun Yat-sen University, Guangzhou 510275, China.

Open Access Article. Published on 27 January 2020. Downloaded on 2/21/2026 1:43:14 AM.
This article is licensed under a Creative Commons Attribution-NonCommercial 3.0 Unported Licence.

Optimization of culture conditions

The culture conditions could be classified to two kinds, liquid culture media and solid culture media. The main component of liquid culture media was water while the solid one was rice. Considering that salt might affect the osmotic pressure of cells and alter the metabolism, and the supplement with amino acids might induce marine fungi to produce diverse alkaloids, the key cultivation parameter alteration was whether having salt and amino acids or not. Detail composition of each nutrient source in the different culture media can see the ESI Table S1.† The LC-MS prescreening of their culture extracts indicated that fungus *Aspergillus* sp. XBB-4 could produce most diverse metabolites in culture medium D (GPY + amino acids) composed of glucose 15 g, peptone 10 g, yeast extract 2 g, L-lysine 2 g, phenylalanine 2 g, L-threonine 2 g, L-tryptophan 2 g, L-methionine 2 g, nicotinamide 1 g, folic acid 1 g, and sea salt 30 g in 1 L water (ESI Fig. S51†). Therefore, culture medium D was selected to ferment this fungus for scale-up production.

Culture method

Aspergillus sp. XBB-4 was cultured in liquid medium D (GPY + amino acids). Fungal mycelia were cut and transferred aseptically to 1000 mL conical flasks each containing 400 mL sterilized liquid medium. The fungus was static incubated at 25 °C for 30 days.

Extraction and isolation

The mycelia and liquid culture (100 L) were separated by cheesecloth. The culture broth was extracted successively three times with EtOAc (60 L) and concentrated by low-temperature rotary evaporation to obtain a crude extract (45.1 g).

The crude extract was subjected to a silica gel chromatography (column diameter: 8 cm, length: 70 cm, silica gel: 500 g) with a gradient of petroleum ether–EtOAc (10 : 0–0 : 10, v/v) followed by EtOAc–MeOH (10 : 0–0 : 10, v/v) to afford 40 fractions (Fr. 1–Fr. 40). Fr. 29 was purified by silica gel column in a step gradient elution with EtOAc–MeOH (10 : 0–0 : 10, v/v) to get 10 sub-fractions (Fr. 29-1–Fr. 29-10). Fr. 29-6 was further purified by reversed-phase silica gel column chromatography using MeOH–H_2O (50 : 50–100 : 0, v/v) gradient elution to obtain Fr. 29-6-1–Fr. 29-6-4. Then Fr. 29-6-3 was further purified by RP-HPLC using MeOH–H_2O (60 : 40, v/v) as the eluent to obtain compound **1** (4.9 mg). Compound **8** (2.6 mg) was obtained from Fr. 29-6-4 by Sephadex LH-20 gel column chromatography and RP-HPLC eluted with MeOH–H_2O (60 : 40, v/v). Compounds **2** (1.9 mg) and **9** (2.3 mg) were gained as the result of the purification of Fr. 29-2 through RP-HPLC with a solvent system methanol–water (70 : 30, v/v). Compound **3** (8.9 mg) was obtained by the natural precipitation of component Fr. 24. HPLC purification of Fr. 29-3 with a solvent system MeOH–H_2O (70 : 30, v/v) gave compound **4** (6.5 mg). Fr. 30 was purified by RP HPLC with an eluent of MeOH–H_2O (70 : 30, v/v) to afford compound **5** (3.0 mg). Fr. 20 was separated by RP-HPLC eluted with MeOH–H_2O (70 : 30, v/v) to obtain sub-fractions Fr. 20-1–Fr. 20-3, and then Fr. 20-2 was further separated by RP-HPLC in MeOH–H_2O (70 : 30, v/v) to afford compound **6** (58.0 mg). Similarly, compound **11** (5.0 mg) was isolated by the further RP-HPLC separation of Fr. 20-3. Fr. 14 and Fr. 15 was merged after ^{1}H NMR prescreening, and then were purified with HPLC using MeOH–H_2O (75 : 25, v/v) as eluent to obtain compound **7** (6.2 mg). Compound **10** (11.3 mg) was gained as white powder from the precipitation of Fr. 4. Fr. 21 was subjected to a reversed-phase silica gel column chromatography using a step gradient of MeOH–H_2O (50 : 50–100 : 0, v/v) as eluent to furnish four sub-fractions Fr. 21-1–21-4, and then Fr. 21-3 was purified by Sephadex LH-20 gel column chromatography eluted with 100% methanol to give compound **12** (2.9 mg). Fr. 25 was purified on RP-HPLC using MeOH–H_2O (80 : 20, v/v) as eluent to obtain compound **13** (7.2 mg).

Aspercarboline A (1). Brown oil; $[\alpha]_D^{25}$ = +1.5 (*c* 0.65, MeOH). UV (MeOH) λ_{max} nm (log ε): 235 (3.16). ECD (0.08 mM, MeOH) λ_{max} ($\Delta\varepsilon$) 317 (+0.57), 210 (−3.14) nm. IR ν_{max}: 3326, 2970, 2934, 1626, 1537, 1448, 1405, 1252, 1084, 999 cm^{-1}. ^{1}H and ^{13}C NMR data see Table 1. HR-ESI-MS at *m*/*z* 243.11268 $[M + H]^+$ (calcd for $C_{14}H_{15}O_2N_2$, 243.11280).

Aspercarboline B (2). White powder; $[\alpha]_D^{25}$ = +60.0 (*c* 0.25, MeOH). UV (MeOH) λ_{max} nm (log ε): 216 (3.12). IR ν_{max}: 3390, 2961, 2918, 1716, 1667, 1624, 1323, 1266, 1206, 1064, 1018, 805, 741 cm^{-1}. ^{1}H and ^{13}C NMR data see Table 1. HR-ESI-MS at *m*/*z* 283.10891 $[M + H]^+$ (calcd for $C_{16}H_{15}N_2O_3$, 283.10772).

Aspercarboline C (3). White powder; $[\alpha]_D^{25}$ = +84.6 (*c* 0.20, MeOH). UV (MeOH) λ_{max} nm (log ε): 235 (3.12). ECD (0.07 mM, MeOH) λ_{max} ($\Delta\varepsilon$) 290 (+3.99), 212 (−3.71) nm. IR ν_{max}: 3320, 1672, 1624, 1432, 1323, 1203, 1124, 1011, 937, 839, 738 cm^{-1}. ^{1}H and ^{13}C NMR data see Table 1. HR-ESI-MS peak at *m*/*z* 285.12302 $[M + H]^+$ (calcd for $C_{16}H_{17}N_2O_3$, 285.12337).

Asperdione A (13). Colorless crystals; $[\alpha]_D^{25}$ = +10.0 (*c* 0.60, MeOH). UV (MeOH) λ_{max} nm (log ε): 318 (4.51). ECD (0.07 mM, MeOH) λ_{max} ($\Delta\varepsilon$) 238 (+2.96), 316 (−0.65) nm. IR ν_{max}: 3299, 2973, 2938, 1662, 1630, 1434, 1384, 1337, 1305, 1280, 1198, 1034, 949, 902, 788 cm^{-1}. ^{1}H and ^{13}C NMR data see Table 2. HR-ESI-MS peak at *m*/*z* 275.15079 $[M + H]^+$ (calcd for $C_{14}H_{19}N_4O_2$, 275.15025).

Absolute configurations of compounds 1, 3 and 13

The absolute configurations of compounds **1**, **3** and **13** were determined by experimental and calculated ECD spectra. The calculated ECD spectra of compounds **1**, **3** and **13** were obtained using the TDDFT method at the PBE1PBE/6-311++G (d, p) level in methanol. Additionally, the ECD spectra were generated from dipole-length dipolar and rotational strengths using a Gaussian band shape with a 0.3 eV exponential half-width and elaborated using the SpecDis program.

X-ray crystal data of compound 13

Crystals of **13** were obtained as colorless crystals from a MeOH solution. Crystal X-ray diffraction data for **13** were collected on a Bruker SMART APEX CCD using graphite-monochromated Cu Kα radiation (λ = 1.54178 Å) at room temperature. Its structure was solved by direct methods (SHELXS-97), expanded using difference Fourier techniques, and *a* = 27.726(2) Å, *b* =

 This journal is © The Royal Society of Chemistry 2020

Open Access Article. Published on 27 January 2020. Downloaded on 2/21/2026 1:43:14 AM.
This article is licensed under a Creative Commons Attribution-NonCommercial 3.0 Unported Licence.

14.7975(12) Å, c = 7.8558(11) Å, V = 3223.0(6) Å^3, Z = 64, d = 1.419 g cm^{-3}. The data were processed using CrysAlis. The thermal ellipsoids are plotted at 30% probability level. The water molecule O1W resides on a 2-fold axis. The carbon atoms C-16 and C-17 exhibit two-fold disorder and only the most probable orientations are shown in the figure for clarity. Crystallographic data of **13** has been deposited with the Cambridge Crystallographic Data Centre (CCDC number 1969177).

Cytotoxicity assay

Human nasopharyngeal carcinoma cell lines CNE1, CNE2, SUNE1 and HONE1 and hepatocellular carcinoma cell lines HepG2 and QGY7701 were generously provided by Professor Mu-Sheng Zeng (Cancer Center, Sun Yat-sen University) and conserved in State Key Laboratory of Oncology in South China, Cancer Center, Sun Yat-sen University, Guangzhou, P. R. China. The culture medium was DMEM (Gibco) with 10% fetal bovine serum (FBS) (Gibco). All of the cells were authenticated using short tandem repeat profiling, tested for Mycoplasma contamination, and cultured for less than 2 months.

The *in vitro* cytotoxicities of **1–13** were determined by means of the colorimetric 3-(4,5-dimethylthiazol-2-yl)-2,5-diphenyl-2*H*-tetrazolium bromide (MTT) assay. The tested human cancer cell lines at a density of 1.5 × 10^7 cells per L and were seeded in 96-well plates. Compounds at different concentrations (1.5625–100 μM) were added to the cultures and then 0.5 mg mL^{-1} MTT was added to the culture medium after 72 h. After incubated for 4 h at 37 °C, the supernatant of the plates was removed. The formazan crystals were dissolved in DMSO (150 μL), and the absorbance was measured at 570 nm by using a microplate reader (Bio-Rad, Hercules, CA, USA), and the data were analyzed with the CalcuSystem software package.

Conclusions

In summary, 13 alkaloids including three new β-carboline alkaloids aspercarbolines A–C (**1–3**), one new piperazinedione, asperdione A (**13**) and nine known alkaloid compounds were obtained from a geoduck *Panopea abbreviate* associated fungus *Aspergillus* sp. XBB-4 by amino acid-directed strategy. The optimization of culture conditions presented the importance of amino acids and salt in inducing the production of alkaloids especially β-carboline alkaloids from fungus. Aspercarboline C (**3**) and asperdione A (**13**) exhibited significant cytotoxic activity against human nasopharyngeal carcinoma cell lines CNE1, CNE2, HONE1 and SUNE1, human hepatocellular carcinoma cell lines hepG2 and QGY7701. The biosynthetic pathways of compounds **1–3** were also proposed. This work provides a feasible way to explore the potential of fungal biosynthesis which can enrich natural product compound library and provide lead compounds for potential drugs development.

Conflicts of interest

There are no conflicts to declare.

Acknowledgements

This work was financed by the National Natural Science Foundation of China (No. 81872795), Guangdong Provincial Science and Technology Research Program (No. 2016A020222004 and 2019B070702003), Natural Science Foundation of Guangdong Province (No. 2018A030313157), and the National Science and Technology Major Project for New Drug Innovation and Development (No. 2017ZX09305010).

References

1 E. K. Lund, *Food Chem.*, 2013, **140**, 413–420.
2 L. L. Fu, C. Wang, Y. Zhu and Y. B. Wang, *Trends Food Sci. Technol.*, 2019, **88**, 80–92.
3 W. M. Laura, C. R. Malco, P. K. Joseph, L. Mark, F. P. Margaret, S. Mary and L. K. Alan, *Innovative Food Sci. Emerging Technol.*, 2005, **6**, 257–270.
4 P. C. Zaidman and E. Morsan, *Fish. Res.*, 2015, **172**, 423–431.
5 M. Goman, B. L. Ingram and A. Strom, *Quat. Int.*, 2008, **188**, 117–125.
6 W. Liu, C. M. Pearce, R. S. McKinley and I. P. Forster, *Aquaculture*, 2016, **452**, 326–341.
7 M. K. Liu, C. B. Wang, L. F. Kong and Q. Li, *Mar. Sci.*, 2013, **37**, 103–106.
8 H. J. Li, Y. L. Xie, Z. L. Xie, Y. Chen, C. K. Lam and W. J. Lan, *Mar. Drugs*, 2012, **10**, 627–638.
9 L. H. Huang, Y. X. Chen, J. C. Yu, J. Yuan, H. J. Li, W. Z. Ma, R. K. Watanapokasin, C. Hu, S. I. Niaz, D. P. Yang and W. J. Lan, *Org. Lett.*, 2017, **19**, 4888–4891.
10 M. X. Yuan, Y. Qiu, Y. Q. Ran, G. K. Feng, R. Deng, X. F. Zhu, W. J. Lan and H. J. Li, *Mar. Drugs*, 2019, **17**, 77.
11 E. Couladouros, A. Magos and A. Strongilos, Greek Patent, GR 1004602 B1 20040618, 2004.
12 P. Phainuphong, V. Rukachaisirikul, S. Saithong, S. Phongpaichit, J. Sakayaroj, C. Srimaroeng, A. Ontawong, A. Duangjai, P. Muangnil and C. Muanprasat, *Bioorg. Med. Chem.*, 2018, **26**, 4502–4508.
13 N. Aimi, M. Kitajima, N. Oya, W. Nitta, H. Takayama, S. Sakai, I. Kostenyuk, Y. Gleba, S. Endress and J. Stockigt, *Chem. Pharm. Bull.*, 1996, **44**, 1637–1639.
14 H. Zhao, Q. L. Wang, S. B. Hou and G. Chen, *J. Nat. Prod.*, 2019, **33**, 2359–2362.
15 Y. Li, M. Zhao and K. L. Parkin, *J. Agric. Food Chem.*, 2011, **59**, 2332–2340.
16 S. Mohamed, S. Dirk, A. S. Khaled, H. Elisabeth, G. W. Iris, W. D. Irene and L. Hartmut, *Rev. Latinoam. Quim.*, 2007, **35**, 58–67.
17 M. L. Yang, P. C. Kuo, T. L. Hwang and T. S. Wu, *J. Nat. Prod.*, 2011, **74**, 1996–2000.
18 N. Yang, Y. H. Shi, A. Z. Xiong, Y. Zhou, L. H. Gu, R. Wang, L. Yang and Z. T. Wang, *J. Sep. Sci.*, 2018, **41**, 3014–3021.
19 D. S. Lee, S. H. Eom, S. Y. Jeong, H. J. Shin, J. Y. Je, E. W. Lee, Y. H. Chung, Y. M. Kim, C. K. Kang and M. S. Lee, *Environ. Toxicol. Pharmacol.*, 2013, **35**, 171–177.
20 Y. L. Cui, N. Shen, J. Dang, L. J. Mei, Y. D. Tao and Z. G. Liu, *J. Sep. Sci.*, 2017, **40**, 2895–2905.

Open Access Article. Published on 27 January 2020. Downloaded on 2/21/2026 1:43:14 AM.
This article is licensed under a Creative Commons Attribution-NonCommercial 3.0 Unported Licence.

21 W. H. Jiao, H. Gao, C. Y. Li, G. X. Zhou, S. Kitanaka, A. Ohmurae and X. S. Yao, *Magn. Reson. Chem.*, 2010, **48**, 490–495.
22 B. Proksa, D. Uhrin, M. Sturdikova and J. Fuska, *Acta Biotechnol.*, 1990, **10**, 337–340.
23 S. Diem and M. Herderich, *J. Agric. Food Chem.*, 2001, **49**, 5473–5478.
24 J. J. Maresh, L. A. Giddings, A. Friedrich, E. A. Loris, S. Panjikar, B. L. Trout, J. Stockigt, B. Peters and S. E. O'Connor, *J. Am. Chem. Soc.*, 2008, **130**, 710–723.
25 Q. Chen, S. F. Zhang and Y. C. Xie, *J. Biotechnol.*, 2018, **281**, 137–143.
26 Q. Chen, C. T. Ji, Y. X. Song, H. B. Huang, J. Y. Ma, X. P. Tian and J. H. Ju, *Angew. Chem., Int. Ed.*, 2013, **52**, 9980–9984.
27 W. Yu. Zhao, W. Y. Zhou, J. J. Chen, G. D. Yao, B. Lin, X. B. Wang, X. X. Huang and S. J. Song, *Phytochemistry*, 2019, **159**, 39–45.
28 H. J. Li, W. J. Lan, C. K. Lam, F. Yang and X. F. Zhu, Hirsutane sesquiterpenoids from the marine-derived fungus *Chondrostereum* sp., *Chem. Biodivers.*, 2011, **8**, 317–324.
29 F. Yang, W. D. Chen, R. Deng, H. Zhang, J. Tang, K. W. Wu, D. D. Li, G. K. Feng, W. J. Lan, H. J. Li, X. F. Zhu and A. Hirsutanol, A novel sesquiterpene compound from fungus *Chondrostereum* sp., induces apoptosis and inhibits tumor growth through mitochondrial-independent ROS production: hirsutanol A inhibits tumor growth through ROS production, *J. Transl. Med.*, 2013, **11**, 32.
30 F. Yang, W. D. Chen, R. Deng, D. D. Li, K. W. Wu, G. K. Feng, H. J. Li and X. F. Zhu, Hirsutanol A induces apoptosis and autophagy *via* reactive oxygen species accumulation in breast cancer MCF-7 cells, *J. Pharmacol. Sci.*, 2012, **119**, 214–220.

 This journal is © The Royal Society of Chemistry 2020